

Exome sequencing of healthy phenotypic extremes links *TROVE2* to emotional memory and PTSD

Angela Heck^{1,2,3*}, Annette Milnik^{1,2,3}, Vanja Vukojevic^{1,2,4}, Jana Petrovska^{1,2}, Tobias Egli^{1,2}, Jochen Singer^{5,6}, Pablo Escobar^{6,7,8}, Thierry Sengstag^{6,7,8}, David Coynel^{2,9}, Virginie Freytag^{1,2}, Matthias Fastenrath^{2,9}, Philippe Demougin^{1,2,4}, Eva Loos^{2,9}, Francina Hartmann^{1,2}, Nathalie Schick Tanz^{2,9}, Bernardo Delarue Bizzini^{1,2,4}, Christian Vogler^{1,2,3}, Iris-Tatjana Kolassa¹⁰, Sarah Wilker¹⁰, Thomas Elbert¹¹, Torsten Schwede^{6,7,8}, Christian Beisel⁵, Niko Beerenwinkel^{5,6}, Dominique J.-F. de Quervain^{2,3,9†} and Andreas Papassotiropoulos^{1,2,3,4*†}

Many mental disorders represent the extremes of the normal distribution of traits, which are related to multiple cognitive and emotional dimensions. By performing whole-exome sequencing of healthy, young subjects with extremely high versus extremely low aversive memory performance, we identified *TROVE2* as a gene implicated in emotional memory in health and disease. *TROVE2* encodes Ro60, a broadly expressed RNA-binding protein implicated in the regulation of inflammatory gene expression and autoimmunity. A regulatory *TROVE2* variant was linked to higher emotional memory capacity and higher emotional memory-related brain activation in healthy subjects. In addition, *TROVE2* was associated with traumatic memory and the frequency of post-traumatic stress disorder in genocide survivors.

Enhanced memory for emotional events, a common observation in animals and humans, is an evolutionary important trait, because it helps remembering both dangerous and favorable situations¹. On the other hand, strong sensory and emotional memories of various life-threatening and aversive experiences may contribute to the development and symptoms of post-traumatic stress disorder (PTSD)^{2,3}, especially when such memories lose their association with the original contextual system^{4,5}. In healthy humans, emotionally charged memory (that is, enhanced memory for emotional events) shows large phenotypic variability⁶ and has been linked to genetic variants of well-established neuromodulatory systems and molecules in candidate gene studies^{6–13}. Similarly, there is substantial variability in the individual vulnerability to develop PTSD, particularly at lower levels of trauma exposure, which can be partially explained by genetic factors¹⁴.

Next-generation sequencing coupled with efficient DNA capture has recently enabled the use of whole-exome sequencing (WES) for the study of the genetics of human phenotypes¹⁵. Indeed, WES studies have been particularly successful at identifying functional variants related to complex traits^{15–17}. Such variants can be identified through extreme-phenotype sampling followed by deep WES^{17–20}. In extreme-phenotype sampling, samples from a carefully selected population at one or both ends of the extremes of a phenotype, which have been adjusted for known covariates, are subjected to sequencing. In these populations, causal variants are expected to be enriched. Thus, even small sample sizes may be

sufficient to suggest candidate variants that can subsequently be genotyped in a larger group of phenotyped individuals, as has also been shown recently by empirical research²¹.

Here we performed WES in healthy, young subjects with extreme high or extreme low emotionally charged memory performance, followed by targeted genotyping in a larger population, which showed a normal distribution of the phenotype of interest ($n = 2,684$). Genotype-dependent differences in emotional memory-related brain activation were studied in a homogenous sub-sample of 1,258 subjects. In addition, we assessed the effect of the identified variants on gene expression in the post-mortem human brain and on symptoms and frequency of PTSD in genocide survivors.

Results

Exome sequencing in phenotypic extremes. WES was performed in 88 healthy, young participants with extreme high or extreme low aversive memory performance carefully matched for sex (1-to-1 matching), genetic background, age and smoking behaviour (see Methods, Fig. 1, Supplementary Fig. 1 and Supplementary Table 1). Aversive memory was quantified by means of a picture delayed free-recall task. High and low extremes were defined on the basis of the distribution of aversive memory performance in $n = 3,418$ healthy, young subjects (see Methods).

WES was performed with the SureSelectXT human all exon V5+UTR target-enrichment kit (Agilent), which allows sequencing of exonic and near-gene regulatory variants. To avoid discarding

¹Division of Molecular Neuroscience, Department of Psychology, University of Basel, CH-4055 Basel, Switzerland. ²Transfaculty Research Platform Molecular and Cognitive Neurosciences, University of Basel, CH-4055 Basel, Switzerland. ³Psychiatric University Clinics, University of Basel, CH-4055 Basel, Switzerland. ⁴Department Biozentrum, Life Sciences Training Facility, University of Basel, CH-4056 Basel, Switzerland. ⁵Department of Biosystems Science and Engineering, ETH Zurich, CH-4058 Basel, Switzerland. ⁶SIB Swiss Institute of Bioinformatics, CH-4056 Basel, Switzerland. ⁷Department Biozentrum, University of Basel, CH-4056 Basel, Switzerland. ⁸sciCORE Center for Scientific Computing, University of Basel, CH-4056 Basel, Switzerland. ⁹Division of Cognitive Neuroscience, Department of Psychology, University of Basel, CH-4055 Basel, Switzerland. ¹⁰Clinical & Biological Psychology, Institute of Psychology & Education, Ulm University, D-89069 Ulm, Germany. ¹¹Department of Psychology, University of Konstanz, D-78457 Konstanz, Germany. [†]These authors jointly supervised this work. *e-mail: angela.heck@unibas.ch; andreas.papas@unibas.ch

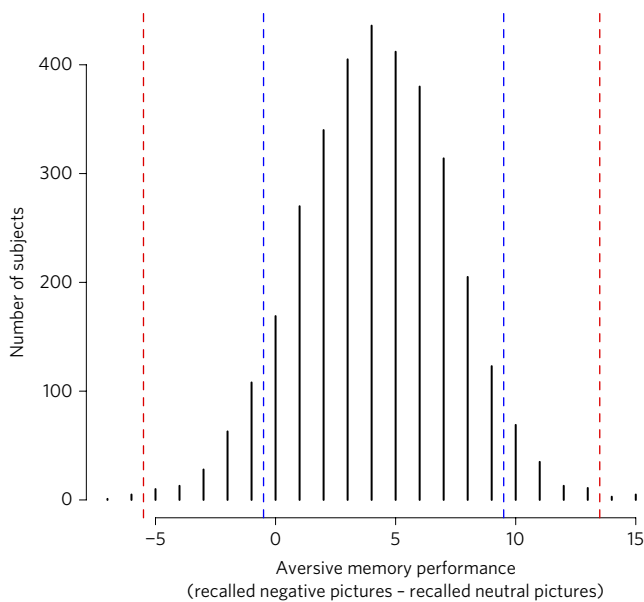


Figure 1 | Frequency histogram of aversive memory performance in 3,418 healthy, young adults. Dotted vertical blue and red lines at the right distribution tail represent the lower and upper performance margins of subjects, respectively, defined as high extremes. Dotted vertical blue and red lines at the left distribution tail represent the upper and lower performance margins of subjects, respectively, defined as low extremes.

variants that were enriched at high frequencies in the extremes²¹, the empirical minor allele frequency (MAF) in the extreme dataset of $n = 88$ subjects was set to ≤ 0.125 (see Methods). Given that no prior information is available regarding putative differences in effect sizes of variants associated with the phenotype of interest, gene-based analyses were done using both burden and adaptive burden tests (see Methods). After adjustment for multiple testing, *TROVE2* (encoding TROVE domain family member 2; also known as Sjögren syndrome type A antigen; Ro60 kDa autoantigen), *PKD2L2* (encoding polycystin 2 like 2, also known as transient receptor potential cation channel), and *CFAP57* (also known as *WDR65*; encoding cilia and flagella associated protein 57) were significantly associated with group membership, which reflected extreme aversive memory performance (Table 1). We investigated *TROVE2* further, because this gene exceeded the adjusted significance threshold in both the burden and adaptive burden test (Table 1). In the burden test, *TROVE2* remained significant after Bonferroni correction for the entire number of genes ($n = 21,175$) that were analysed in the burden test ($P_{\text{nominal}} = 2 \times 10^{-6}$, $P_{\text{Bonferroni}} = 0.042$; Supplementary Fig. 2). Moreover, *TROVE2* was the best hit ($P_{\text{nominal}} = 0.0002$) in the optimized sequence kernel association test (SKAT-O)²² (Supplementary Table 2). A detailed view of the sequencing data for *TROVE2* (Fig. 2) showed that the variant, which is mainly responsible for the results of the gene burden tests, was a 3'-UTR (untranslated region) single-nucleotide polymorphism (SNP) (rs72740218; C/T transition on chr1:193054088 according to GRCh37/hg19 coordinates). Notably, 10 of the 44 high-extreme individuals were heterozygous minor T allele carriers, whereas this was only the case for 2 of the 44 low-extreme individuals. Pyrosequencing-based genotyping confirmed this result (see Methods). According to the Exome Aggregation Consortium (ExAC) browser (version 0.3.1), rs72740218 MAF is 0.08 in European (non-Finnish) populations.

Free-recall performance for positive material relative to neutral material (termed positive memory, in analogy to aversive memory) was also significantly higher in high-extreme subjects. However, this was entirely owing to this group's lower free-recall performance

for neutral pictures (Supplementary Table 1). The genetic association findings were unrelated to the difference in positive memory between extreme groups. Firstly, *TROVE2* was not significant ($P = 0.6$) when tested at the gene level (SKAT-O with positive memory as the quantitative phenotype). Secondly, *TROVE2*-variant rs6692342 was not significantly associated with positive memory ($P = 0.2$) or with free recall for positive pictures ($P = 0.9$).

Next, we tested whether the association of the T allele with increased aversive memory performance could also be detected in the entire population of healthy young subjects ($n = 2,684$ successfully genotyped for rs72740218, including the $n = 88$ sequenced subjects, see Methods). We identified 19 minor allele homozygotes, 369 heterozygotes, and 2,296 major allele homozygotes (empirical MAF = 0.075, Hardy-Weinberg $P > 0.1$). The T allele was significantly correlated ($P = 0.005$) with increased aversive memory performance, also after exclusion of the $n = 88$ sequenced extremes ($P = 0.035$, $n = 2,596$). This sample of $n = 2,596$ participants consisted of $n = 217$ subjects that had not been selected for exome sequencing, but nonetheless fulfilled the performance criteria for extreme high or extreme low aversive memory (Supplementary Table 3), and of 2,379 non-extreme individuals. Notably, the significant association between rs72740218 and aversive memory performance in this population of $n = 2,596$ participants was attributable to subjects that exhibited extreme aversive memory performance ($P = 0.0008$ for the interaction 'genotype X extreme/non-extreme group membership'; $r = 0.11$ in $n = 217$ non-sequenced extremes; $r = 0.016$ in $n = 2,379$ non-extremes).

Functional brain imaging. In the next step, we used functional brain imaging (functional magnetic resonance imaging, fMRI) to identify *TROVE2* rs72740218-dependent differences in brain activity related to memory encoding of aversive stimuli in $n = 1,258$ subjects, a sub-sample of the population of $n = 2,596$ healthy subjects (sequenced extremes were excluded), who participated in the behavioural genetic study. All neuroimaging data were acquired in the same MRI scanner, thereby reducing hard- and software-related methodological variance.

We first investigated encoding-related brain activation independently of whether the information was later recalled or not (see Methods). We found significant ($P < 0.05$, two-sided test, family-wise error (FWE) corrected for the whole brain (P_{FWE})) gene dose-dependent (that is, with increasing number of the minor T allele) activity increases in the middle frontal gyrus, Brodmann area 9 (peak at ((-33, 36, 48), $t = 5.39$; $P_{\text{FWE}} = 0.0015$)) (Supplementary Fig. 3). Because these activation differences may be independent of memory processes, we then investigated brain activation that was related to successful memory encoding, that is, activation that was specifically related to information that was later recalled (see Methods). We observed significant positive associations between the *TROVE2* genotype (with increasing number of the minor T allele) and aversive memory-related activity in the left medial prefrontal cortex (peak at (-5.5, 38.5, 36), superior frontal gyrus/paracingulate gyrus, Brodmann area 32, $t = 5.80$; $P_{\text{FWE}} = 0.0003$; with FWE-corrected voxels extending to the dorsal anterior cingulate) (Fig. 3 and Supplementary Fig. 4). Even after excluding the 6 minor allele homozygotes from the analysis, we still found significant *TROVE2*-dependent differences in activation between the major allele homozygotes and the heterozygotes with the peak at the same coordinate ((-5.5, 38.5, 36), $t = 5.25$; $P_{\text{FWE}} = 0.0125$). There were no significant increases in activity with increasing number of major alleles. Additionally, we tested whether the reported association was specific for the negative valence. An analysis of *TROVE2*-dependent differences in brain activity, which were related to successful memory encoding of positive stimuli compared to neutral stimuli (see Methods), did not show significant FWE-corrected results; nevertheless the corresponding uncorrected significance level was

Table 1 | Results of gene-based analyses in phenotypic extremes.

Gene symbol	Gene name	Burden test P Value		Adaptive burden test P value	
		Nominal	Adjusted*	Nominal	Adjusted*
<i>TROVE2</i>	<i>TROVE</i> domain family member 2 (also known as Sjögren syndrome type A antigen, Ro60 kDa autoantigen)	2×10^{-6}	0.0004	4×10^{-5}	0.004
<i>PKD2L2</i>	Polycystin 2 like 2, transient receptor potential cation channel	0.00022	0.045	0.00288	0.317
<i>CFAP57</i>	Cilia and flagella associated protein 57	0.00026	0.053	0.00035	0.038

*Corrected for the number of genes reaching i -stat < 0.001 in the respective test (burden test: 203 genes; adaptive burden test: 110 genes).

high ($(-5.5, 38.5, 36)$, $t = 3.44$; $P_{\text{uncorrected}} = 0.0006$; $P_{\text{FWE}} = 0.97$). Accordingly, we did not observe significant ($P < 0.05$, two-sided test, FWE-corrected for the whole brain) associations between the number of minor *TROVE2* alleles and contrast testing for differences in brain activity between successful memory encoding of aversive compared to positive stimuli (see Methods), suggesting that, although the observed association was strongest for aversive stimuli, it was also observable for the positive valence.

In summary, the fMRI experiment showed that the minor allele of *TROVE2* SNP rs72740218, which was associated with increased memory for aversive information, was also related to increased brain activity in the medial prefrontal cortex during successful memory encoding of emotional pictures, whereby the strongest association was observed for aversive ones.

***TROVE2* expression in human frontal cortex.** Given the effect of the *TROVE2* minor allele on brain activation that is related to successful memory encoding in the prefrontal cortex, we further investigated possible minor-allele effects on *TROVE2* expression in this part of the human brain. For this analysis, we used the BRAINEAC data, a publicly available resource for the exploration of the regulatory significance of genetic variants in the human brain (<http://www.braineac.org/>)²³. Brain samples specified as frontal cortex probes in the BRAINEAC database were taken from the prefrontal cortex²⁴, mostly Brodmann area 9/46, a region well-known for its involvement in emotional processing and emotional memory^{25,26}. The 3'-UTR variant rs72740218 was significantly associated with

expression of the adjacent *TROVE2* terminal coding exon (exon-specific probeset 2372955; chr1:193053788–193053828, GRCh37/hg19 coordinates) in the prefrontal cortex of 125 deceased subjects. The minor T allele predisposed to significantly higher expression values ($P = 0.005$, Fig. 4a), possibly suggesting a local effect of this variant on expression of the corresponding exon. No significance was observed at the full-transcript level (that is, the Winsorized means over all exon-specific probesets) (Supplementary Table 4).

***TROVE2* genetic variability in traumatized survivors of the Rwandan genocide.** Extremely aversive, in particular life-threatening, incidents can lead to an excessive and persisting emotional memory of the traumatic events, which can result in intrusive and distressing re-experiencing (traumatic memory), a core PTSD symptom. The heritability of re-experiencing traumatic events ranges from 23% to 51%, suggesting that naturally occurring genetic variations have an important effect on this trait²⁷. Given the association of *TROVE2* with aversive memory and aversive memory-related brain activation in healthy subjects, we hypothesized that *TROVE2* would also be associated with emotional memory for traumatic events reflected in increased re-experiencing symptoms. We tested this hypothesis in 271 refugees who have fled from the Rwandan civil war, who have been living in the Nakivale refugee camp in Uganda during the time of investigation, and from whom lifetime data on the prevalence of PTSD were available (137 females; 134 males; mean age, 35 years; range, 18–68 years; see Methods). All subjects had experienced highly aversive situations and were examined

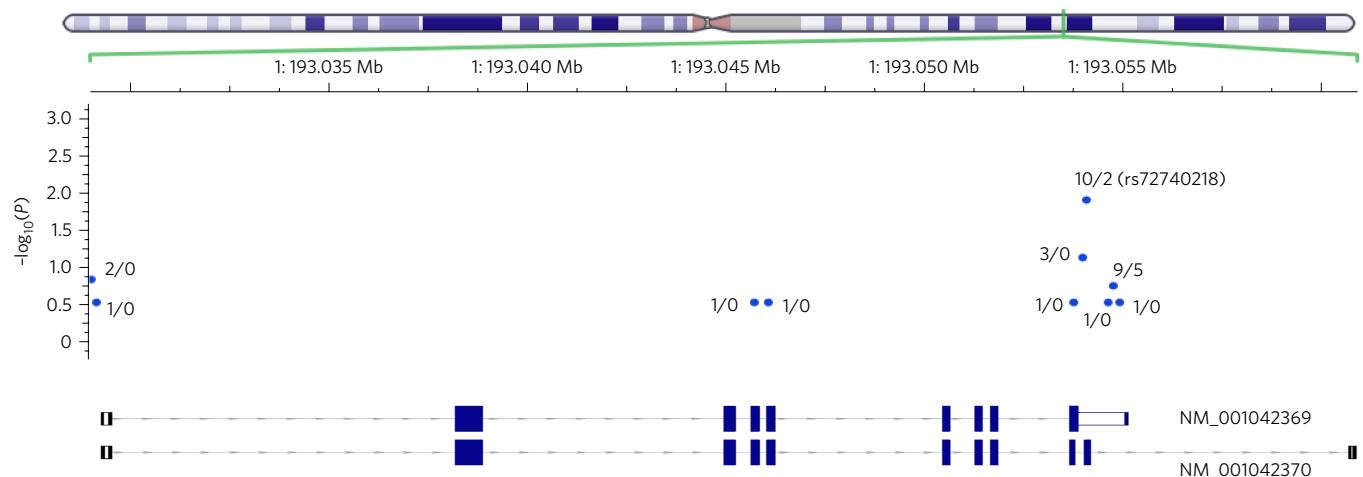


Figure 2 | Sequencing results of *TROVE2* (positions according to the GRCh37/hg19 coordinates). Blue dots indicate variants with MAF ≤ 0.125 detected in the sample of 88 individuals with extreme aversive memory performance. Solidus-separated numbers accompanying each dot indicate the frequency of the occurrence of the respective minor allele in subjects with extremely high and extremely low performance (high/low). The minor allele of variant rs72740218 was observed in 10 high extremes and in 2 low extremes. The y axis indicates $-\log_{10}$ of the P value of genetic association tests that were performed separately for each variant. For illustration purposes, two *TROVE2* transcript variants (see also Fig. 4) are shown in the lower part of the figure. Blue filled rectangles represent coding exons, empty rectangles represent non-coding exons and UTRs.

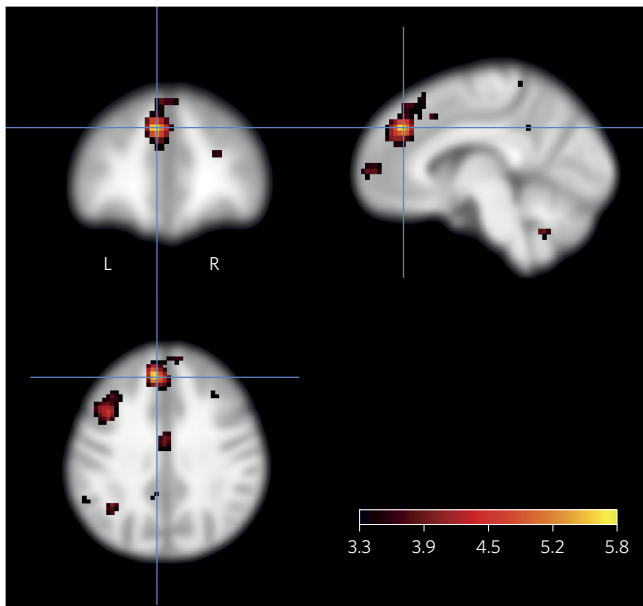


Figure 3 | *TROVE2* rs72740218 genotype-dependent differences in brain activity related to successful memory encoding of aversive stimuli compared with neutral stimuli in 1,258 healthy young subjects. Displayed are positive associations between genotype (the number of minor T alleles) and activity. The blue cross indicates the peak genotype-dependent activation ($t = 5.80$; $P_{\text{FWE}} = 0.0003$) in the left medial prefrontal cortex at $(-5.5, 38.5, 36)$. Activations are overlaid on coronal, sagittal and axial sections of brain images, displayed at $t \geq 3.1$ ($P_{\text{nominal}} < 0.001$) and using colour-coded t values. L, left side of the brain; R, right side of the brain.

by trained experts with a structured interview based on the Post-traumatic Diagnostic Scale²⁸ with the help of trained interviewers chosen from the refugee community. Traumatic events were assessed using a checklist of 36 reported war- and non-war-related traumatic event types (such as, injury by a weapon, rape, accidents) (Supplementary Table 5). In sub-Saharan African samples, the rs72740218 variant is rare (MAF < 0.01 , according to dbSNP). Therefore, we analysed all *TROVE2*-spanning common SNPs that were present on the Human SNP Array 6.0 with an empirical MAF ≥ 0.05 in the Rwandan sample ($n = 5$ tagging SNPs, Table 2). None of these variants was significantly associated with age, sex, the number of experienced traumatic event types, or with the occurrence of any of the 36 distinct traumatic event types (Table 2 and Supplementary Table 5). *TROVE2* SNPs were significantly associated with traumatic memory (that is, lifetime symptoms of re-experiencing the traumatic event) and with frequency of lifetime PTSD (Table 2). Variant rs6692342, which is located 555 and 1,007 bases upstream of the respective *TROVE2* transcript variants (Fig. 5), showed the strongest association: the minor allele G was associated with increased traumatic memory ($P = 0.007$) and with increased PTSD frequency ($P = 0.0004$). Linkage disequilibrium between variants rs6692342 and rs72740218 was not calculated in the PTSD sample, given the very low frequency of rs72740218 in the Rwandan population. In the healthy, young population sample, variants rs72740218 and rs6692342 were unlinked ($r^2 = 0.02$). Because the occurrence of some of the traumatic event types was unevenly distributed between rs6692342 genotype groups (albeit without reaching corrected statistical significance; Supplementary Table 5), we reran the analyses by controlling for such uneven distributions and obtained nearly identical results (Supplementary Table 6). The minor allele G of variant rs6692342 was also moderately associated with increased expression of the adjacent *TROVE2* non-coding exon 1 of transcript variants NM_004600, NM_001173525,

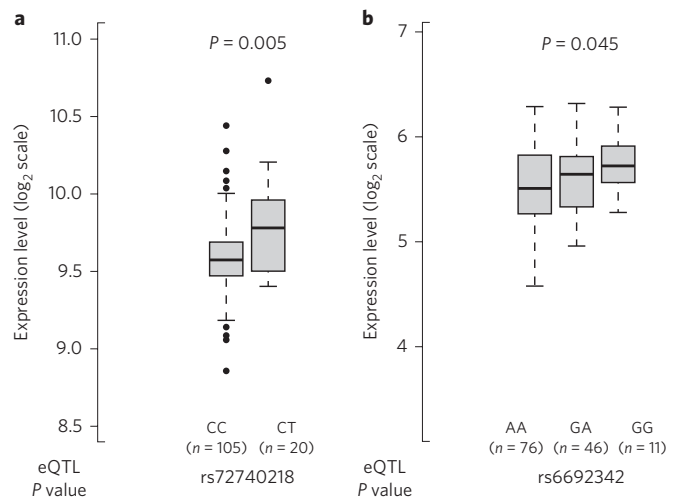


Figure 4 | Association of *TROVE2* SNPs rs72740218 and rs6692342 in the human frontal cortex. **a, b,** Association of *TROVE2* SNPs rs72740218 (**a**) and rs6692342 (**b**) with gene expression. **a,** Expression values of exon-specific probeset 2372955 (chr1:193053788–193053828). **b,** Expression values of exon-specific probeset 2372928 (chr1:193028950–193029112; GRCh37/hg19 coordinates). Data and box plots were retrieved from the BRAINEAC project server²³ (<http://www.braineac.org/>, accessed on 7 October 2016). Box plots demarcate the 25th and 75th percentile (middle line is median), and bars represent the minimum and maximum values. Filled circles represent outliers. eQTL, expression quantitative trait locus.

NM_001042369 and NM_001042370 (exon-specific probeset 2372928, chr1:193028950–193029112, GRCh37/hg19 coordinates) in the prefrontal cortex of 123 deceased subjects of the BRAINEAC study ($P = 0.045$, Fig. 4b), possibly suggesting a local effect of this variant on expression of the corresponding exon. No significance was observed at the full-transcript level (that is, the Winsorized means over all exon-specific probesets) (Supplementary Table 4). The frequency of the minor G allele of rs6692342 was nearly identical in the BRAINEAC and Rwandan samples (25.6% and 24.6%, respectively). Accordingly, genotype frequencies of rs6692342 did not differ between these samples ($P = 0.5$, χ^2 test). Notably, genotype and allele frequencies in the BRAINEAC and Rwandan samples for rs6692342 were in close agreement with the reported values for European and Sub-Saharan populations, respectively, in the 1000 genomes project (Phase 3).

Discussion

The present study suggests that variants related to increased expression of *TROVE2* transcripts in the human frontal cortex are linked to emotional memory capacity and emotional memory-related brain activation in healthy subjects, and to traumatic memory and risk for PTSD in traumatized genocide survivors.

TROVE2 is widely expressed in human tissues, including the brain and its frontal cortex^{23,29}. *TROVE2* undergoes complex transcriptional regulation, such as alternative splicing with several coding transcript variants and a range of 8–11 coding and non-coding exons^{30,31} (Fig. 5). SNP rs72740218 was associated with emotional memory performance and brain activation related to successful memory encoding of emotionally charged information in the medial prefrontal cortex, one of the key brain regions related to emotional processing³², although it does not belong to one of the typical localizations found to be activated by emotional memory encoding in genotype-independent studies³³. It is important to note, however, that genotype-independent analyses may not reveal brain regions for which different genotype groups show opposite activation patterns, for example when major-allele

Table 2 | Associations between common *TROVE2* SNPs and traumatic memory (P_{memory}), lifetime PTSD (P_{PTSD}), sex (P_{sex}), age (P_{age}), and the number of traumatic event types (P_{events}).

SNP ID	Localization	MAF	P_{sex}	P_{age}	P_{events}	P_{memory}	P_{PTSD}
rs6692342	Upstream	0.25	0.868	0.952	0.712	0.007	0.0004
rs4657842	Upstream	0.35	0.895	0.328	0.652	0.191	0.023
rs7554496	Intronic	0.15	0.323	0.800	0.318	0.169	0.581
rs10801173	3'-UTR; intronic	0.47	0.235	0.316	0.746	0.186	0.024
rs41520747	Downstream; intronic	0.18	0.360	0.669	0.791	0.587	0.017

homozygotes show a deactivation, whereas the other genotype groups show an activation, as was the case with SNP rs72740218 (Supplementary Fig. 5). Notably, it has been shown that PTSD patients, when compared to controls, have an increased response in the left dorsal anterior cingulate/medial prefrontal cortex at

almost identical coordinate positions (peak at -3, 39, 39) during encoding of later remembered negative verbal information³⁴. Of note, there is evidence for a dissociative subtype of PTSD patients, who typically show increased activation in the anterior cingulate/medial prefrontal cortex³⁵.

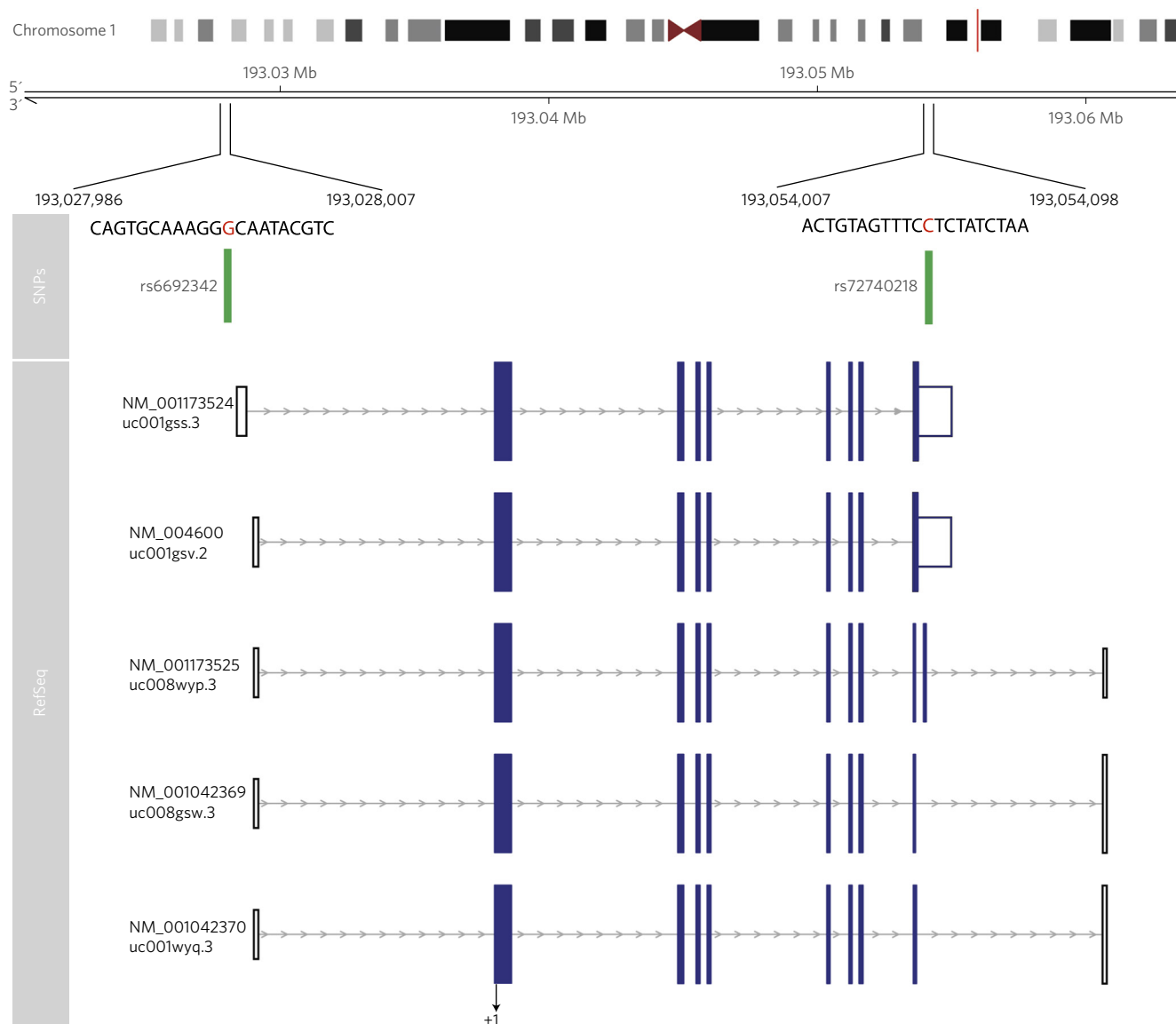


Figure 5 | Schematic representation of selected *TROVE2* RefSeq transcript variants (positions according to GRCh37/hg19 coordinates). UCSC (University of California Santa-Cruz) identifiers are also given beneath each RefSeq identifier. Blue filled rectangles represent coding exons, empty rectangles represent non-coding exons and UTRs. SNPs rs6692342 and rs72740218 are zoomed in with 10 bases up- and downstream; +1: first coding base in the first coding exon.

SNP rs72740218 is located within the 3'-UTR of transcripts NM_001173524 and NM_004600 (Fig. 5), and is significantly associated with expression levels of the terminal coding exon of these variants in the prefrontal cortex (Fig. 4). SNP rs6692342, which was associated with traumatic memory and PTSD frequency, is located 555 bases upstream of transcript variant NM_001173524 and 1,007 bases upstream of transcript variants NM_004600, NM_001173525, NM_001042369, and NM_001042370, and is moderately, albeit significantly associated with expression levels of the adjacent non-coding exon 1 of the latter four variants in the prefrontal cortex (Fig. 4). Taken together, the minor alleles of these *TROVE2* SNPs were associated with increased expression of adjacent exons and with gain of emotional (in the case of rs72740218) and traumatic (in the case of rs6692342) memory-related phenotypes. Given that free recall was assessed shortly after encoding in this study, further research will be needed to study the role of this gene on emotional memory capacity related to the longer-term (such as, hours, days) consolidation processes.

TROVE2 encodes Ro60, an RNA-binding protein that binds to misfolded, non-coding RNAs, pre-5S rRNA (ribosomal RNA) and Y RNA (small non-coding RNA)³¹. Autoantibodies to Ro60 are prevalent in autoimmune disorders including Sjögren's syndrome and systemic lupus erythematosus^{36–38}, and recent research supports the idea of a direct link between Ro60 autoantibody production, type I interferon, and autoimmunity³⁹. The findings of the present study support a genetic link between *TROVE2* and emotional memory-related traits, possibly by regulation of specific transcripts. Although speculative, one might hypothesize that *TROVE2* has a role in a possible link between the regulation of immune-related processes and the regulation of emotional memory-related traits, given the crucial involvement of *TROVE2* in autoimmunity. Notably, recent genetic and epidemiological data point to a link between autoimmunity and PTSD: a retrospective cohort study of 666,269 Iraq and Afghanistan veterans revealed significant associations between PTSD and risk for autoimmune disorders, whereby shared etiology was one of the possible explanations for this observation⁴⁰. Recently, a large genome-wide association study (GWAS) of PTSD has shown a significantly increased enrichment ratio for immune-related expression quantitative trait loci in PTSD⁴¹. In addition, abnormal cytokine regulation and a proinflammatory milieu are present in PTSD^{42–45}. Thus, a link between the regulation of immune functions and emotional memory-related neuropsychiatric phenotypes probably exists. Despite the known, direct connection between the human brain and peripheral tissues relevant to the function of the immune system⁴⁶, it is not yet possible to draw any causal inferences about the mechanistic nature of this link and about a putative involvement of *TROVE2*. Notably, recent animal research identified meningeal immunity as a direct player in the regulation of complex brain functions, such as learning, memory and social behaviour^{47,48}.

A number of—mostly small—PTSD GWAS in civilian and military or veteran samples have been published^{41,49–55}. *TROVE2* has not been reported as one of the top hits in these GWAS. Of note, the published GWAS results do not converge so far. It is widely acknowledged that substantial within- and between-sample differences in traumatic event type, duration and rate, time of trauma onset, ancestry, sociodemographic factors and social support render comparability of GWAS results in the PTSD field inherently difficult⁵⁶. The possibility exists that some of the reported findings might prove specific to a certain population. Therefore, the replication issue of genetic studies of PTSD will remain challenging and might be resolved by future large collaborative efforts, which should include different subgroups of large homogenous samples. Notably, a recent study that has reported on combined genetic and transcriptomic findings in human and *C. elegans* identified *TROVE2* as one of the top scoring genes involved in mood regulation and stress response⁵⁷.

In the present study, we used exome sequencing in healthy phenotypic extremes to detect genes that were linked to emotionally charged memory capacity. Notably, the extreme phenotype design proved to be essential for the identification of *TROVE2*, because the effect size of the minor allele T of rs72740218 was considerably higher in the extremes, also in the non-sequenced samples, compared to the largest, middle part of the phenotypic distribution. It is important to stress that the success of the genetic search presented herein is not necessarily generalizable to every genetically complex cognitive and/or emotional trait. A synergy of factors, such as meticulous matching of phenotypic extremes with a particular focus on genetic background¹⁵, a relatively high MAF for the implicated variant and the specific genetic architecture of the phenotype of interest, gave rise to the identification of *TROVE2*. Nevertheless, our experience with this approach and the statistical features of our findings are in close analogy to the observations of a recent study, which identified a genetic modifier of a Mendelian trait (cystic fibrosis) by means of exome sequencing in phenotypic extremes²¹.

In conclusion, *TROVE2*, a gene implicated in autoimmunity, is linked to emotionally charged memory in health and psychiatric disease, particularly in PTSD. Specifically, the present findings suggest that the drawback of the *TROVE2* variant-related enhancement of emotional memory is increased enhancement of intrusive and distressing memory for traumatic events. Given that many mental disorders represent the extremes of a normal distribution of traits on multiple cognitive and emotional dimensions⁵⁸, we believe that appropriate genetic methodologies in healthy phenotypic extremes may help uncover disease dimensions with different symptom patterns, a subtyping that may be necessary to improve understanding and treatment of psychopathology.

Methods

Definition of phenotypic extremes. Aversive memory was assessed in $n = 3,418$ subjects who participated in ongoing behavioural and imaging genetics studies of healthy, young adults in the city of Basel, Switzerland (data lock April 2015). The ethics committee of the Cantons of Basel-Stadt and Basel-Landschaft approved the experiments. All participants received general information about the study and gave their written, informed consent for participation. Participants were free of any neurological or psychiatric illness, and did not take any medication at the time of the experiment (except hormonal contraceptives).

Aversive memory was quantified by means of a picture delayed free-recall task. Stimuli consisted of 72 pictures that were selected from the International Affective Picture System⁵⁹, as well as from in-house standardized picture sets that allowed us to equate the pictures for visual complexity and content (such as human presence). On the basis of normative valence scores (from 1 to 9), pictures were assigned to emotionally negative (2.3 ± 0.6), emotionally neutral (5.0 ± 0.3), and emotionally positive (7.6 ± 0.4) conditions, resulting in 24 pictures for each emotional valence. Four additional pictures that showed neutral objects were used to control for primacy and recency effects in memory. Two of these pictures were presented at the beginning and two at the end of the picture task. These pictures were not included in the analysis. The pictures were presented for 2.5 s in a quasi-randomized order. To ensure that the ratio between valence categories was kept constant across consecutive parts of the entire picture sequence, each twelfth part of the sequence contained exactly two positive, two negative and two neutral pictures. Thus, maximally four pictures of the same category occurred consecutively. Ten minutes after picture presentation, memory performance was tested using a free-recall task, which required participants to write down a short description (a few words) of the previously seen pictures. Remembered primacy and recency pictures as well as training pictures were excluded from the analysis. No time limit was set for this task. A picture was scored as correctly recalled, if the rater could identify the presented picture on the basis of the subject's description. Two trained investigators rated the descriptions independently for recall success (inter-rater reliability >99%). A third independent rater decided on those pictures that had been rated differently⁷. For the purpose of selecting phenotypic extremes, aversive memory performance was calculated by subtracting the number of the freely recalled neutral pictures from the number of freely recalled negative pictures. In a sub-sample of 1,900 subjects with data on a second assessment of free-recall performance 24 h after the first presentation of the identical picture set, both phenotypes showed high levels of inter-trial correlation (Pearson's $r = 0.73$ and $r = 0.78$ for free recall of negative and neutral pictures, respectively). On the basis of the observed phenotypic distribution, subjects with aversive memory performance ≥ 10 and ≤ 13 were classified as high-extreme subjects (HES), and subjects with aversive memory performance ≥ -5 and ≤ -1 were classified as

low-extreme subjects (LES). We adopted an almost-extreme sampling approach, because the very extremes of cognitive phenotypes are vulnerable to potential measurement errors and phenotype heterogeneity¹⁸. For example, performance at the very extreme low end of the distribution might be related to erroneous understanding of task instructions or to gross errors in task execution. Moreover, the additive polygenic mode of inheritance of common phenotypes breaks down at the very extremes of the distribution tails^{60,61}. Thus, subjects at the very extreme ends, as identified upon visual inspection of the frequency histogram (that is, aversive memory performance < -5 , $n = 6$; aversive memory performance > 13 , $n = 8$), were not considered for further analysis (Fig. 1).

Next, we selected all subjects who had been genotyped on the Genome-Wide Human SNP Array 6.0 (Affymetrix) and performed standard quality control with PLINK (<https://atgu.mgh.harvard.edu/plinkseq/>) including sex check and identity by descent analysis as described in ref.⁶², resulting in $n = 2,991$ subjects with quality-controlled SNP array data.

The next steps were performed to calculate each subject's genetic background, to select a homogeneous group of participants of European ancestry, and to compute an individual parameter in order to match the to-be-sequenced extremes for genetic similarity. Thus, we analysed the SNP array data of seven Swiss and German samples^{62–64} (total $n = 5,172$) including our target sample. Genetic data of these subjects was projected onto the first two principal components (PCs) of genetic variation in the HapMap3 reference sample (consisting of African, Asian and European samples) using SMARTPCA⁶⁵. Participants scoring for PC1 < 0.012 and for PC2 < 0.065 were then filtered out to obtain a cluster of broad European ancestry (Supplementary Fig. 1a, b). Genetic data of the subjects composing this cluster was also checked for the presence of duplicates and cryptic relatedness (identity by descent: $\hat{p} < 0.2$). Before performing the final principal component analysis within this European sample, genetic quality control (MAF > 0.02 , call rate > 0.95 , Hardy–Weinberg $P > 0.001$) was applied within each of the seven sub-samples separately. We also excluded SNPs within regions of long-range linkage disequilibrium as has been suggested in ref.⁶⁶. The remaining autosomal SNPs of the combined sample were then pruned using PLINK (indep-pairwise command; window-size 200 SNPs, 5 SNP steps, $r^2 < 0.2$). We next used SMARTPCA⁶⁵ to estimate the PCs of genetic variation within this broad European cluster (Supplementary Fig. 1a, b). The resulting first two PCs were used as parameters for genetic similarity.

After these steps, $n = 2,739$ subjects of European ancestry remained for further selection of pairs of subjects from the high- and low extreme groups that: (1) have a similar genetic background; (2) have the same sex; (3) were investigated at a similar time point; (4) are of similar age; (5) have similar smoking behaviour. The latter matching criterion was included given the borderline significant correlation between smoking status and being a member of the high or low extreme performance group ($P = 0.08$ before matching). Matching was done separately for females and males with the library Matching (Version 4.8–3.4) in R⁶⁷. Membership in the low or high extreme group was used as treatment vector. Matching was done without replacement, the sequence of the subjects entering the matching procedure was chosen randomly. Time point of investigation, age, smoking behaviour and the two results of the first two PCs from the genetic similarity analysis were used as variables to match on. For each HES, the best-matching LES was identified, separately for females and males. Finally, these high extreme–low extreme pairs were randomly assigned on the plate for subsequent exome sequencing. In line with the circumstance that emotionally arousing information is often remembered at the expense of neutral background information⁶⁸, HES had significantly increased mean free-recall performance for aversive pictures ($P = 3 \times 10^{-17}$) and significantly, albeit orders of magnitude weaker, decreased mean free-recall performance for neutral pictures ($P = 1 \times 10^{-12}$) than LES (Supplementary Table 1). No difference in mean free-recall performance for positive pictures ($P = 0.6$) was observed between HES and LES. Overall memory capacity was very similar between extreme groups ($P = 0.5$). No significant group difference in arousal and valence ratings for any of the 3 picture categories was observed (all comparisons: $P > 0.05$).

Exome sequencing: blood sampling, DNA isolation and related quality controls. Blood samples were collected between midday and evening (mean time of day: 14:30, range 13:00–20:00) using BD Vacutainer Push Button blood collection sets and 10.0-mL BD Vacutainer Plus plastic whole blood tubes, BD Hemogard closure with spray-coated K₂EDTA (Becton, Dickinson and Company, New Jersey, USA). Standard haematological analysis, including blood-cell counting, was performed with a Sysmex pocH-100i Automated Hematology Analyzer (Sysmex Co, Kobe, Japan.) DNA was isolated from the remaining fraction, upon plasma removal. The isolation was performed with the QIAmp Blood Maxi Kit (Qiagen AG, Hilden, Germany), using the recommended spin protocol. In order to obtain high purity DNA, isolated DNA samples were additionally re-purified. For this purpose, 2 μ g of DNA isolated with the QIAmp/Oragene procedure, was incubated overnight at 50 °C with proteinase K (lysis buffer: 30 mM TrisCl, 10 mM EDTA, 1% SDS pH 8.0, 150 ng μ l⁻¹ Proteinase K), agitated by gentle orbital shaking. Next, DNA was purified using the Genomic DNA Clean & Concentrate Kit (Zymo Research, Irvine, California, USA). The quality and concentration of DNA were assessed using gel electrophoresis,

NanoDrop ND-1000 (Thermo Scientific, Waltham, Massachusetts, USA) and fluorometry measurements (Qubit dsDNA BR Assay Kit; Invitrogen, Carlsbad, California, USA), respectively. DNA samples of high integrity and purity were further normalized to 24 ng μ l⁻¹ and randomly assigned to a 96-well plate for library preparation.

Exome sequencing: library preparation. Quality checks of the genomic DNA samples and intermediate products of the library preparation (efficiency of DNA fragmentation, pre- and post-capture libraries) were done with the Fragment Analyzer, using the DNF-467 Genomic DNA 50 kb Analysis Kit and DNF-473 Standard Sensitivity NGS Fragment Analysis Kit, respectively (Advanced Analytical Technologies, Ankeny, Iowa, USA). Library preparation for WES was performed with the Agilent SureSelectXT Human All Exon V5+UTR kit using the SureSelectXT automated target enrichment for Illumina paired-end multiplexed sequencing protocol on the Agilent NGS workstation, option B (Agilent Technologies Inc, Santa Clara, California, USA). In brief, 200 ng of genomic DNA was fragmented with the Covaris E220 focused-ultrasonicator (Covaris Inc, Woburn, Massachusetts, USA), with the following settings: duty factor: 10%; peak incident power: 175; cycles per burst: 200; treatment time: 360 s; bath temperature: 4–8 °C. The target DNA fragment size was 150–200 bp. After quality assessment the libraries were further prepared by using the SureSelect XT Library Prep Kit ILM (Agilent, USA; SureSelectXT target enrichment system for Illumina paired-end multiplexed sequencing library protocol version B3). AMPure XP bead purification was always implemented between the library preparation steps. First, the 3' ends of the DNA fragments were adenylated, followed by paired-end adaptor ligation and adaptor-ligated library amplification. After library quality assessment, samples were hybridized to the target-specific capture library and the hybridized DNA was captured with streptavidin-coated beads. The libraries with 8-bp indexing primers were then amplified, assayed for quality and quantity and finally pooled for multiplexed sequencing.

Whole-exome sequencing. Libraries were clustered on the Illumina cBot cluster station (HiSeq PE Cluster Kit v4). WES was done on an Illumina HiSeq 2500 machine (paired-end reads, 101 bp per read). The libraries were mixed in 4 pools ($3 \times 24 + 1 \times 22$). Each pool was sequenced in 6 lanes. A fifth pool was mixed with 27 of the samples and this Pool 5 was sequenced in an extra lane. For each sample, over 12 Gb of sequence were generated.

The SureSelectXT Human All Exon V5+UTR kit (Agilent) used in this study targets 359,555 exons in 21,522 genes (that is, 75 Mb of sequence) included in the following databases: CCDS, RefSeq, GENCODE, miRBase, TCGA and UCSC. The sequence of each sample was mapped to the hg19 human reference genome, downloaded from <http://genome.ucsc.edu>, using BWA 0.7.12 (Burrow–Wheeler Alignment)⁶⁹. Duplicates were flagged with Picard 1.135 (<http://picard.sourceforge.net>). Analysis of coverage was done with Picard CalculateHSMetrics and Bedtools⁷⁰ version 2.18.1. Finally, 98% of the target bases had a coverage equal or greater than 20 \times and approximately 50% of target bases had 100 \times coverage (Bedtools; Supplementary Fig. 6). Base quality score recalibration and local realignment around indels was done with GATK⁷¹ version 3.4-0 following the standard GATK protocol⁷². Single nucleotide variants (SNVs) were called with the Haplotype Caller. No padding was used for variant calling outside non-target regions to prevent false-positive SNV calls. Following the recommendation of ref.⁷³, variant quality score recalibration was used. We chose 99% sensitivity for a variant to be 'true' on the basis of an adaptive error model and filtered out false-positive variants using this threshold.

Exome sequencing: callset quality control. The final callset was evaluated using variant-level concordance (that is, the percentage of variants in the study sample that matched a defined gold standard) and genotype concordance (that is, the percentage of variants that matched the genotypes derived from the same samples using a different genotyping technique). After defining dbSNP 138.b37 as the gold standard, we ran the VariantEval toolkit of GATK. The variant-level concordance rate between our callset and dbSNP was high (98.33%). Two genotype concordance measures can be derived from comparing sequencing data with array data: non-reference sensitivity (NRS, that is, the rate at which non-reference alleles in the array data are also identified in the sequenced genotypes) and the non-reference discrepancy (NRD; that is, the rate at which sequenced genotypes differ from array genotypes) rate. We used the GATK toolkit GenotypeConcordance for these calculations. 18,709 bi-allelic overlapping variants were identified for both WES data and array genotype data of the Affymetrix 6.0 human SNP array. NRS was 97.5%, suggesting a high sensitivity for common variants, and NRD was 2.4%. The ratio between transitions to transversions (T_i/T_v ratio) was 2.61, which matched the expected value of 2.5–2.8 well, for sequences covering both exonic and non-exonic 3' and 5' UTRs⁷⁴, like the SureSelectXT Human All Exon V5+UTR kit (Agilent), which targets 75 Mb of the human genome. We furthermore checked the rate of novel missense SNPs (that is, not included in dbSNP 138.b37) in our callset. The mean over all samples was low ($n = 57.8$), suggesting a low number of false-positive calls. Another quality indicator is the het/hom ratio (that is, the ratio between heterozygous and homozygous

non-reference variants). In our casset, the het/hom ratio, which is expected to be approximately 1.5 for European populations^{75,76}, was 1.57 for all SNPs and 1.54 for known SNPs (that is, dbSNP SNPs). Variant call format data were annotated with the reference genome GRCh37.75 using SnpEff software version 4.11 (build 2015-10-03)⁷⁷.

Pyrosequencing. Targeted genotyping of *TROVE2* SNP rs72740218 was done with pyrosequencing on a PyroMark ID System. The following primers were used: 5'-TACTAACTAGCTCTTGGGAAAT-3' (forward primer, 5'-biotinylated), 5'-CAAAGCAAACATTTTACAGTGT-3' (reverse primer), 5'-CAAAAAGTTCTCTATTAGAT-3' (sequencing primer). $n = 2,684$ subjects were successfully genotyped for rs72740218. One-sided genetic-association testing (additive model) was used for hypothesis confirmation purposes. Researcher team members involved in genotyping were blinded to group allocation.

Burden testing. Genotype–phenotype associations were calculated with PLINK/SEQ version 0.10 (<https://atgu.mgh.harvard.edu/plinkseq/>). We calculated gene-based tests falling into two categories: burden tests⁷⁸ and adaptive burden tests (variable threshold test)⁷⁹. Burden tests perform optimally when assuming that a large proportion of variants are causal and the effects are in the same direction. Adaptive burden tests, which use data-adaptive weights or thresholds, are thought to be more robust than burden tests that use fixed weights or thresholds⁸⁰. Following power analyses done in studies of phenotypic extremes with similar sample size as in the present one, we set the empirical MAF as $MAF \leq 0.125$ to avoid eliminating variants enriched to high frequency in the extremes²¹. To correct for multiple testing we used the *i*-stat statistic (that is, the smallest possible empirical *P* value of a gene), which is implemented in PLINKSeq. According to previous recommendations¹⁵, the *i*-stat threshold was set to <0.001 . Burden-test-derived significances were then Bonferroni-corrected for the number of genes with an *i*-stat below this threshold.

fMRI experiment. Subjects were right-handed, free of any lifetime neurological or psychiatric illness, and did not take any medication (except hormonal contraceptives) at the time of the experiment, which was approved by the ethics committee of the Cantons of Basel-Stadt and Basel-Landschaft. Written, informed consent was obtained from all subjects before participation. After receiving general information about the study and giving their informed consent, participants were instructed and then trained on the picture task they later performed in the scanner. After training, they were positioned in the scanner. The participants received earplugs and headphones to reduce scanner noise. Their head was fixated in the coil using small cushions, and they were told not to move their heads. Functional magnetic resonance images were acquired during the performance of the picture task in two separate sessions (total scanning time, approximately 30 min). After finishing the tasks, participants left the scanner and were taken to a separate room for free recall of the pictures. Finally, participants filled out questionnaires, gave saliva for genotype analysis and were debriefed. The total length of the experimental procedure was approximately 3 hours. We excluded 54 subjects from the fMRI experiment. Reasons for exclusion were defined as follows: corrupted or missing data ($n = 40$), subjects recalling less than one picture in one of the valence categories ($n = 10$), failed co-registration ($n = 4$).

Measurements were performed on a Siemens Magnetom Verio 3 T wholebody MR unit equipped with a twelve-channel head coil. Functional time series were acquired with a single-shot echo-planar sequence using parallel imaging (GRAPPA). We used the following acquisition parameters: TE (echo time) = 35 ms, FOV (field of view) = 22 cm, acquisition matrix = 80×80 , interpolated to 128×128 , voxel size: $2.75 \times 2.75 \times 4$ mm³, GRAPPA acceleration factor $R = 2.0$. Using a midsagittal scout image, 32 contiguous axial slices were placed along the anterior–posterior commissure (AC–PC) plane covering the entire brain with a TR = 3,000 ms ($\alpha = 82^\circ$). The first two acquisitions were discarded owing to T_1 saturation effects. A high-resolution T_1 -weighted anatomical image was acquired using a magnetization prepared gradient echo sequence (MPRAGE, TR = 2,000 ms; TE = 3.37 ms; TI = 1,000 ms; flip angle = 8; 176 slices; FOV = 256 mm; voxel size = $1 \times 1 \times 1$ mm³).

Preprocessing and data analysis was performed using SPM8 (Statistical Parametric Mapping, Wellcome Department of Cognitive Neurology, London, UK; <http://www.fil.ion.ucl.ac.uk/spm/>) implemented in Matlab (Mathworks Inc., Natick, Massachusetts, USA). Volumes were slice-time corrected to the first slice and realigned to the first acquired volume. Both functional and structural images were spatially normalized by applying DARTEL, which leads to an improved registration between subjects. Normalization incorporated the following steps: (1) Structural images of each subject were segmented using the 'New Segment' procedure in SPM8. (2) The resulting gray- and white-matter images were used to derive a study-specific group template. The template was computed from a subpopulation of 1,000 subjects from this study. (3) An affine transformation was applied to map the group template to MNI space. (4) Subject-to-template and template-to-MNI transformations were combined to map the functional images to MNI space. The functional images were smoothed with an isotropic 8 mm full width at half maximum Gaussian filter. Serial correlations were removed

using a first-order autoregressive model. A high-pass filter (128 s) was applied to remove low-frequency noise.

Normalized functional images were masked using information from their respective T_1 anatomical file as follows: a partial volume effect file obtained from the SPM-VBM8 toolbox (<http://dbm.neuro.uni-jena.de/vbm8/>) was used as a starting point to define the brain mask. This volume represents the three-tissue classification results of the segmentation process (GM, WM, CSF), with two additional mixed classes (GM–WM, GM–CSF). It was binarized, dilated and eroded with a $3 \times 3 \times 3$ voxels kernel using fslmaths (FSL) to fill in potential small holes in the mask. The previously computed DARTEL flowfield was used to normalize the brain mask to MNI space, at the spatial resolution of the functional images. The mask was finally thresholded at 10% and applied to the normalized functional images. Consequently, the implicit intensity-based masking threshold usually that was employed to compute a brain mask from the functional data during the first level specification (by default fixed at $mask.thresh = 0.8$) was not needed any longer and set to a lower value of 0.05.

For each subject, analyses were conducted in the framework of the general linear model. Regressors, which modelled the onset and duration of stimulus events, were convolved with a canonical haemodynamic response function. More precisely, the model comprised regressors for button presses that were modelled as stick/delta functions, picture presentations that were modelled with an epoch/boxcar function (duration: 2.5 s), and rating scales that were modelled with an epoch/boxcar function of variable duration (depending on when the subsequent button press occurred). Six movement parameters were also entered as nuisance covariates. Pictures accounting for possible primacy and recency effects were modelled separately.

Brain activity contrasts were calculated individually using a fixed-effects model (first level analysis). The following contrasts were specified: (1) brain activity related to memory encoding of aversive stimuli compared to neutral stimuli, independent of whether the information was later recalled or not (aversive pictures – neutral pictures); (2) brain activity related to successful memory encoding of aversive stimuli compared to neutral stimuli (aversive pictures recalled – aversive pictures not recalled) – (neutral pictures recalled – neutral pictures not recalled); (3) differences in brain activity between successful memory encoding of aversive compared to positive stimuli (aversive pictures recalled – aversive pictures not recalled) – (positive pictures recalled – positive pictures not recalled); (4) brain activity related to successful memory encoding of positive stimuli compared to neutral stimuli (positive pictures recalled – positive pictures not recalled) – (neutral pictures recalled – neutral pictures not recalled). The resulting contrast parameters were then used for genotype-dependent analyses in a random-effects model (second level analysis). Specifically, we used a regression model to analyse differences in brain activity, whereas the number of alleles served as covariate in our analysis. We controlled for the effects of sex and age by including them as covariates. Significance peaks were assigned to anatomical labels based on the Harvard–Oxford Cortical Structural Atlas⁸¹. Brodmann areas are given based on ref. ⁸².

Rwanda sample. Study participants were survivors of the Rwandan genocide who were living as refugees in the Nakivale refugee settlement. As the Nakivale refugee settlement has grown over the last decade and is spread over a large area, participants were sampled proportionally to the population size from each zone. To exclude genetic relatives in the samples, only one person per household was interviewed. Interviewees had been trained to detect current alcohol abuse and acute psychotic symptoms; candidates exhibiting these signs were excluded. All subjects had experienced highly aversive traumatic situations (including life-threatening situations) and were examined in 2006/2007 by psychologists of the University of Konstanz with the help of trained interpreters, or by intensely trained local interviewers using a structured interview that was based on the Post-traumatic Diagnostic Scale²⁸ with the help of trained interpreters. This procedure has been validated for implementation in East-African crisis regions⁸³. Traumatic events were assessed with a checklist of 36 war- and non-war-related traumatic event types, such as, injury by weapon, rape, accident, which have also been employed in previous studies⁷. Traumatic load was estimated by assessing the number of different traumatic event types experienced or witnessed. This measure has been shown to be more reliable than assessing the frequency of traumatic events⁸⁴. The procedures and study protocols were approved by the Ethics Committees of the University of Konstanz, Germany, and the Mbarara University of Science and Technology (MUST), Mbarara, Uganda.

Instruments were translated into Kinyarwanda using several steps of translations, blind back-translations, and subsequent corrections by independent groups of translators. Following the translations, the psychometric properties of the translated scales were investigated in a validation study including a retest spanning a two-week period and a cross-validation with expert ratings⁸⁵. To avoid known ceiling effects (that is, the phenomenon that almost everybody will develop PTSD at extreme levels of trauma load)^{86,87}, subjects were selected to have experienced no more than 16 different traumatic event types. Subjects that lacked sufficient data for the estimation of the prevalence of lifetime PTSD were excluded from this study. The significance level of genetic associations with traumatic memory and PTSD risk was calculated by performing forward and backward linear and logistic

regressions, respectively, under inclusion of age, sex, trauma load, and—wherever indicated—occurrence of specific traumatic event types. The significance level of genetic associations with trauma load and the occurrence of specific traumatic events was calculated by performing forward and backward linear and logistic regressions, respectively, under inclusion of age and sex. The significance level of genetic associations with age and sex was calculated by performing linear regressions and χ^2 tests, respectively. Saliva samples were obtained from each person using the Oragen DNA Self-Collection Kit (DNA Genotek, Ottawa, Ontario, Canada). DNA was extracted from saliva using standard protocols.

Data availability. The data that support the findings of this study are available from the corresponding author upon request.

Received 7 October 2016; accepted 27 February 2017;
published 27 March 2017

References

- McGaugh, J. L. In *Memory and Emotion* (Weidenfeld and Nicolson, 2003).
- Pitman, R. K. Post-traumatic stress disorder, hormones, and memory. *Biol. Psychiatry* **26**, 221–223 (1989).
- Phelps, E. A. & LeDoux, J. E. Contributions of the amygdala to emotion processing: from animal models to human behavior. *Neuron* **48**, 175–187 (2005).
- Brewin, C. R., Dalgleish, T. & Joseph, S. A dual representation theory of posttraumatic stress disorder. *Psychol. Rev.* **103**, 670–686 (1996).
- Brewin, C. R., Gregory, J. D., Lipton, M. & Burgess, N. Intrusive images in psychological disorders: characteristics, neural mechanisms, and treatment implications. *Psychol. Rev.* **117**, 210–232 (2010).
- de Quervain, D. J. *et al.* A deletion variant of the $\alpha 2b$ -adrenoceptor is related to emotional memory in Europeans and Africans. *Nat. Neurosci.* **10**, 1137–1139 (2007).
- de Quervain, D. J. *et al.* PKC α is genetically linked to memory capacity in healthy subjects and to risk for posttraumatic stress disorder in genocide survivors. *Proc. Natl Acad. Sci. USA* **109**, 8746–8751 (2012).
- Todd, R. M. *et al.* Deletion variant in the *ADRA2B* gene increases coupling between emotional responses at encoding and later retrieval of emotional memories. *Neurobiol. Learn. Mem.* **112**, 222–229 (2014).
- Todd, R. M., Palombo, D. J., Levine, B. & Anderson, A. K. Genetic differences in emotionally enhanced memory. *Neuropsychologia* **49**, 734–744 (2011).
- Papassotiropoulos, A. *et al.* Human genome-guided identification of memory-modulating drugs. *Proc. Natl Acad. Sci. USA* **110**, E4369–E4374 (2013).
- Ackermann, S., Heck, A., Rasch, B., Papassotiropoulos, A. & de Quervain, D. J. The BclI polymorphism of the glucocorticoid receptor gene is associated with emotional memory performance in healthy individuals. *Psychoneuroendocrinology* **38**, 1203–1207 (2013).
- Gibbs, A. A., Bautista, C. E., Mowlem, F. D., Naudts, K. H. & Duka, T. Alpha 2B adrenoceptor genotype moderates effect of reboxetine on negative emotional memory bias in healthy volunteers. *J. Neurosci.* **33**, 17023–17028 (2013).
- Cheung, J. & Bryant, R. A. FKBP5 risk alleles and the development of intrusive memories. *Neurobiol. Learn. Mem.* **125**, 258–264 (2015).
- Wilker, S., Elbert, T. & Kolassa, I.-T. The downside of strong emotional memories: how human memory-related genes influence the risk for posttraumatic stress disorder—a selective review. *Neurobiol. Learn. Mem.* **112**, 75–86 (2014).
- Kiezun, A. *et al.* Exome sequencing and the genetic basis of complex traits. *Nat. Genet.* **44**, 623–630 (2012).
- Wang, Z., Liu, X., Yang, B. Z. & Gelernter, J. The role and challenges of exome sequencing in studies of human diseases. *Front. Genet.* **4**, 160 (2013).
- Peloso, G. M. *et al.* Phenotypic extremes in rare variant study designs. *Eur. J. Hum. Genet.* **24**, 924–930 (2016).
- Li, D., Lewinger, J. P., Gauderman, W. J., Murcray, C. E. & Conti, D. Using extreme phenotype sampling to identify the rare causal variants of quantitative traits in association studies. *Genet. Epidemiol.* **35**, 790–799 (2011).
- Auer, P. L. & Lettre, G. Rare variant association studies: considerations, challenges and opportunities. *Genome Med.* **7**, 16 (2015).
- Guey, L. T. *et al.* Power in the phenotypic extremes: a simulation study of power in discovery and replication of rare variants. *Genet. Epidemiol.* **35**, 236–246 (2011).
- Emond, M. J. *et al.* Exome sequencing of extreme phenotypes identifies *DCTN4* as a modifier of chronic *Pseudomonas aeruginosa* infection in cystic fibrosis. *Nat. Genet.* **44**, 886–889 (2012).
- Lee, S. *et al.* Optimal unified approach for rare-variant association testing with application to small-sample case-control whole-exome sequencing studies. *Am. J. Hum. Genet.* **91**, 224–237 (2012).
- Ramasamy, A. *et al.* Genetic variability in the regulation of gene expression in ten regions of the human brain. *Nat. Neurosci.* **17**, 1418–1428 (2014).
- Trabzuni, D. *et al.* Quality control parameters on a large dataset of regionally dissected human control brains for whole genome expression studies. *J. Neurochem.* **119**, 275–282 (2011).
- LaBar, K. S. & Cabeza, R. Cognitive neuroscience of emotional memory. *Nat. Rev. Neurosci.* **7**, 54–64 (2006).
- Buchanan, T. W. Retrieval of emotional memories. *Psychol. Bull.* **133**, 761–779 (2007).
- Stein, M. B., Jang, K. L., Taylor, S., Vernon, P. A. & Livesley, W. J. Genetic and environmental influences on trauma exposure and posttraumatic stress disorder symptoms: a twin study. *Am. J. Psychiatry* **159**, 1675–1681 (2002).
- Foa, E. B., Cashman, L., Jaycox, L. & Perry, K. The validation of a self-report measure of posttraumatic stress disorder: The posttraumatic diagnostic scale. *Psychol. Assess.* **9**, 445–451 (1997).
- Hawrylycz, M. J. *et al.* An anatomically comprehensive atlas of the adult human brain transcriptome. *Nature* **489**, 391–399 (2012).
- Spear, M. L. *et al.* The UCSC genome browser database: 2016 update. *Nucleic Acids Res.* **44**, D717–D725 (2016).
- UniProt, C. UniProt: a hub for protein information. *Nucleic Acids Res.* **43**, D204–D212 (2015).
- Etkin, A., Egner, T. & Kalisch, R. Emotional processing in anterior cingulate and medial prefrontal cortex. *Trends Cogn. Sci.* **15**, 85–93 (2011).
- Murty, V. P., Ritchey, M., Adcock, R. A. & LaBar, K. S. fMRI studies of successful emotional memory encoding: a quantitative meta-analysis. *Neuropsychologia* **48**, 3459–3469 (2010).
- Thomae, K. *et al.* Increased anterior cingulate cortex and hippocampus activation in complex PTSD during encoding of negative words. *Soc. Cogn. Affect. Neurosci.* **8**, 190–200 (2013).
- Lanius, R. A. *et al.* Emotion modulation in PTSD: clinical and neurobiological evidence for a dissociative subtype. *Am. J. Psychiatry* **167**, 640–647 (2010).
- Schulte-Pelkum, J., Fritzlter, M. & Mahler, M. Latest update on the Ro/SS-A autoantibody system. *Autoimmun. Rev.* **8**, 632–637 (2009).
- Alspaugh, M. & Maddison, P. Resolution of the identity of certain antigen-antibody systems in systemic lupus erythematosus and Sjogren's syndrome: an interlaboratory collaboration. *Arthritis Rheum.* **22**, 796–798 (1979).
- Clark, G., Reichlin, M. & Tomasi, T. B. Jr. Characterization of a soluble cytoplasmic antigen reactive with sera from patients with systemic lupus erythematosus. *J. Immunol.* **102**, 117–122 (1969).
- Hung, T. *et al.* The Ro60 autoantigen binds endogenous retroelements and regulates inflammatory gene expression. *Science* **350**, 455–459 (2015).
- O'Donovan, A. *et al.* Elevated risk for autoimmune disorders in Iraq and Afghanistan veterans with posttraumatic stress disorder. *Biol. Psychiatry* **77**, 365–374 (2015).
- Stein, M. B. *et al.* Genome-wide association studies of posttraumatic stress disorder in 2 cohorts of US army soldiers. *JAMA Psychiatry* **73**, 695–704 (2016).
- Eraly, S. A. *et al.* Assessment of plasma C-reactive protein as a biomarker of posttraumatic stress disorder risk. *JAMA Psychiatry* **71**, 423–431 (2014).
- Michopoulos, V. *et al.* Association of CRP genetic variation and CRP level with elevated PTSD symptoms and physiological responses in a civilian population with high levels of trauma. *Am. J. Psychiatry* **172**, 353–362 (2015).
- Smith, A. K. *et al.* Differential immune system DNA methylation and cytokine regulation in post-traumatic stress disorder. *Am. J. Med. Genet. B Neuropsychiatr. Genet.* **156B**, 700–708 (2011).
- Lindqvist, D. *et al.* Proinflammatory milieu in combat-related PTSD is independent of depression and early life stress. *Brain Behav. Immun.* **42**, 81–88 (2014).
- Louveau, A. *et al.* Structural and functional features of central nervous system lymphatic vessels. *Nature* **523**, 337–341 (2015).
- Derecki, N. C. *et al.* Regulation of learning and memory by meningeal immunity: a key role for IL-4. *J. Exp. Med.* **207**, 1067–1080 (2010).
- Filiano, A. J. *et al.* Unexpected role of interferon- γ in regulating neuronal connectivity and social behaviour. *Nature* **535**, 425–429 (2016).
- Kilaru, V. *et al.* Genome-wide gene-based analysis suggests an association between Neurologin 1 (*NLGN1*) and post-traumatic stress disorder. *Transl. Psychiatry* **6**, e820 (2016).
- Ashley-Koch, A. E. *et al.* Genome-wide association study of posttraumatic stress disorder in a cohort of Iraq–Afghanistan era veterans. *J. Affect. Disord.* **184**, 225–234 (2015).
- Nievergelt, C. M. *et al.* Genomic predictors of combat stress vulnerability and resilience in U.S. marines: a genome-wide association study across multiple ancestries implicates *PRTFDC1* as a potential PTSD gene. *Psychoneuroendocrinology* **51**, 459–471 (2015).
- Almli, L. M. *et al.* A genome-wide identified risk variant for PTSD is a methylation quantitative trait locus and confers decreased cortical activation to fearful faces. *Am. J. Med. Genet. B Neuropsychiatr. Genet.* **168B**, 327–336 (2015).

53. Logue, M. W. *et al.* A genome-wide association study of post-traumatic stress disorder identifies the retinoid-related orphan receptor alpha (*RORA*) gene as a significant risk locus. *Mol. Psychiatry* **18**, 937–942 (2013).
54. Xie, P. *et al.* Genome-wide association study identifies new susceptibility loci for posttraumatic stress disorder. *Biol. Psychiatry* **74**, 656–663 (2013).
55. Guffanti, G. *et al.* Genome-wide association study implicates a novel RNA gene, the lincRNA *AC068718.1*, as a risk factor for post-traumatic stress disorder in women. *Psychoneuroendocrinology* **38**, 3029–3038 (2013).
56. Logue, M. W. *et al.* The psychiatric genomics consortium posttraumatic stress disorder workgroup: posttraumatic stress disorder enters the age of large-scale genomic collaboration. *Neuropsychopharmacology* **40**, 2287–2297 (2015).
57. Rangaraju, S. *et al.* Mood, stress and longevity: convergence on *ANK3*. *Mol. Psychiatry* **21**, 1037–1049 (2016).
58. Papassotiropoulos, A. & de Quervain, D. J. Failed drug discovery in psychiatry: time for human genome-guided solutions. *Trends Cogn. Sci.* **19**, 183–187 (2015).
59. Lang, P. J., Bradley, M. M. & Cuthbert, B. N. *International Affective Pictures System (IAPS): Affective Ratings of Pictures and Instruction Manual* (Univ. Florida, 2008).
60. Wood, A. R. *et al.* Defining the role of common variation in the genomic and biological architecture of adult human height. *Nat. Genet.* **46**, 1173–1186 (2014).
61. Locke, A. E. *et al.* Genetic studies of body mass index yield new insights for obesity biology. *Nature* **518**, 197–206 (2015).
62. Heck, A. *et al.* Genetic analysis of association between calcium signaling and hippocampal activation, memory performance in the young and old, and risk for sporadic Alzheimer disease. *JAMA Psychiatry* **72**, 1029–1036 (2015).
63. Heck, A. *et al.* Converging genetic and functional brain imaging evidence links neuronal excitability to working memory, psychiatric disease, and brain activity. *Neuron* **81**, 1203–1213 (2014).
64. Hauer, D. *et al.* Relationship of a common polymorphism of the glucocorticoid receptor gene to traumatic memories and posttraumatic stress disorder in patients after intensive care therapy. *Crit. Care Med.* **39**, 643–650 (2011).
65. Price, A. L. *et al.* Principal components analysis corrects for stratification in genome-wide association studies. *Nat. Genet.* **38**, 904–909 (2006).
66. Price, A. L. *et al.* Long-range LD can confound genome scans in admixed populations. *Am. J. Hum. Genet.* **83**, 132–135 (2008); author reply **83**, 135–139 (2008).
67. Sekhon, J. S. Multivariate and propensity score matching software with automated balance optimization: the matching package for R. *J. Stat. Softw.* **42**, 1–52 (2011).
68. Reisberg, D. & Heuer, F. in *Memory and Emotion* (eds Reisberg, D. & Hertel, P.) 3–40 (Oxford Univ. Press, 2004).
69. Li, H. & Durbin, R. Fast and accurate short read alignment with Burrows–Wheeler transform. *Bioinformatics* **25**, 1754–1760 (2009).
70. Quinlan, A. R. & Hall, I. M. BEDTools: a flexible suite of utilities for comparing genomic features. *Bioinformatics* **26**, 841–842 (2010).
71. McKenna, A. *et al.* The genome analysis toolkit: a MapReduce framework for analyzing next-generation DNA sequencing data. *Genome Res.* **20**, 1297–1303 (2010).
72. Van der Auwera, G. A. *et al.* From FastQ data to high confidence variant calls: the Genome Analysis Toolkit best practices pipeline. *Curr. Protoc. Bioinformatics* **43**, 11.10.1–11.10.33 (2013).
73. DePristo, M. A. *et al.* A framework for variation discovery and genotyping using next-generation DNA sequencing data. *Nat. Genet.* **43**, 491–498 (2011).
74. Guo, Y., Ye, F., Sheng, Q., Clark, T. & Samuels, D. C. Three-stage quality control strategies for DNA re-sequencing data. *Brief. Bioinform.* **15**, 879–889 (2014).
75. McKernan, K. J. *et al.* Sequence and structural variation in a human genome uncovered by short-read, massively parallel ligation sequencing using two-base encoding. *Genome Res.* **19**, 1527–1541 (2009).
76. Schuster, S. C. *et al.* Complete Khoisan and Bantu genomes from southern Africa. *Nature* **463**, 943–947 (2010).
77. Cingolani, P. *et al.* A program for annotating and predicting the effects of single nucleotide polymorphisms, SnpEff: SNPs in the genome of *Drosophila melanogaster* strain w¹¹¹⁸; iso-2; iso-3. *Fly* **6**, 80–92 (2012).
78. Madsen, B. E. & Browning, S. R. A groupwise association test for rare mutations using a weighted sum statistic. *PLoS Genet.* **5**, e1000384 (2009).
79. Price, A. L. *et al.* Pooled association tests for rare variants in exon-resequencing studies. *Am. J. Hum. Genet.* **86**, 832–838 (2010).
80. Lee, S., Abecasis, G. R., Boehnke, M. & Lin, X. Rare-variant association analysis: study designs and statistical tests. *Am. J. Hum. Genet.* **95**, 5–23 (2014).
81. Desikan, R. S. *et al.* An automated labeling system for subdividing the human cerebral cortex on MRI scans into gyral based regions of interest. *Neuroimage* **31**, 968–980 (2006).
82. Damasio, H. & Damasio, A. R. *Lesion Analysis in Neuropsychology*, (Oxford Univ. Press, 1989).
83. Ertl, V. *et al.* Validation of a mental health assessment in an African conflict population. *Psychol. Assess.* **22**, 318–324 (2010).
84. Wilker, S. *et al.* How to quantify exposure to traumatic stress? Reliability and predictive validity of measures for cumulative trauma exposure in a post-conflict population. *Eur. J. Psychotraumatol.* **6**, 28306 (2015).
85. Onyut, L. P. *et al.* Trauma, poverty and mental health among Somali and Rwandese refugees living in an African refugee settlement — an epidemiological study. *Confl. Health* **3**, 6 (2009).
86. Kolassa, I.-T., Kolassa, S., Ertl, V., Papassotiropoulos, A. & De Quervain, D. J. The risk of posttraumatic stress disorder after trauma depends on traumatic load and the catechol-o-methyltransferase Val(158)Met polymorphism. *Biol. Psychiatry* **67**, 304–308 (2010).
87. Neuner, F. *et al.* Psychological trauma and evidence for enhanced vulnerability for posttraumatic stress disorder through previous trauma among West Nile refugees. *BMC Psychiatry* **4**, 34 (2004).

Acknowledgements

This work was funded by the University of Basel, the Swiss National Science Foundation (grants 163434, 147570 and 159740 to D.J.-F.d.Q. and A.P.), the European Community's Seventh Framework Programme (FP7/2007–2013) under grant agreement 602450 (IMAGEMEND; grant to A.P. and D.J.-F.d.Q.), the Novartis Foundation for medical-biological Research (grant 15C219 to A.P.), and by the German Research Foundation (Deutsche Forschungsgemeinschaft; grants to I.-T.K. and T.E.). The funders had no role in study design, data collection and analysis, decision to publish or preparation of the manuscript.

Author contributions

A.P., D.J.-F.d.Q., A.H., A.M. and M.F. conceived and designed the study. A.H., A.M., V.V., J.P., T.E.g., J.S., D.C., V.F., M.F., P.D., E.L., F.H., N.S., B.D.B., C.V., I.-T.K., S.W., T.E.L., D.J.-F.d.Q. and A.P. analysed the data. P.E., T.Se., T.Sc., C.B. and N.B. provided bioinformatic support. A.P., A.H. and D.J.-F.d.Q. wrote the manuscript. All authors reviewed and approved the final manuscript.

Additional information

Supplementary information is available for this paper.

Reprints and permissions information is available at www.nature.com/reprints.

Correspondence and requests for materials should be addressed to A.P. or A.H.

How to cite this article: Heck, A. *et al.*, Exome sequencing of healthy phenotypic extremes links *TROVE2* to emotional memory and PTSD. *Nat. Hum. Behav.* **1**, 0081 (2017).

Publisher's note: Springer Nature remains neutral with regard to jurisdictional claims in published maps and institutional affiliations.

Competing interests

The authors declare no competing interests.